

Generating Visually Realistic Adversarial Patch

Xiaosen Wang
Huawei Singular Security Lab
xiaosen@hust.edu.cn

Kunyu Wang
Chinese University of Hong Kong
kunyuwang@link.cuhk.edu.hk

Abstract

Deep neural networks (DNNs) are vulnerable to various types of adversarial examples, bringing huge threats to security-critical applications. Among these, adversarial patches have drawn increasing attention due to their good applicability to fool DNNs in the physical world. However, existing works often generate patches with meaningless noise or patterns, making it conspicuous to humans. To address this issue, we explore how to generate visually realistic adversarial patches to fool DNNs. Firstly, we analyze that a high-quality adversarial patch should be **realistic**, **position irrelevant**, and **printable** to be deployed in the physical world. Based on this analysis, we propose an effective attack called VRAP, to generate visually realistic adversarial patches. Specifically, VRAP constrains the patch in the neighborhood of a real image to ensure the visual reality, optimizes the patch at the poorest position for position irrelevance, and adopts Total Variance loss as well as gamma transformation to make the generated patch printable without losing information. Empirical evaluations on the ImageNet dataset demonstrate that the proposed VRAP exhibits outstanding attack performance in the digital world. Moreover, the generated adversarial patches can be disguised as the scrawl or logo in the physical world to fool the deep models without being detected, bringing significant threats to DNNs-enabled applications.

1. Introduction

With the prosperous development of Deep Neural Networks (DNNs), DNNs have achieved excellent performance in many tasks, *e.g.*, image classification [17, 26], object detection [41, 42], segmentation [33, 43], *etc.* However, Szegedy et al. [46] found that DNNs are vulnerable to adversarial examples, *i.e.*, the maliciously crafted inputs that are indistinguishable from the correctly classified images but can induce misclassification on the target model. Such vulnerability poses significant threats when applying DNNs to security-critical applications, which also attracts broad attention to the security of DNNs [10, 14, 49, 55, 64, 65].

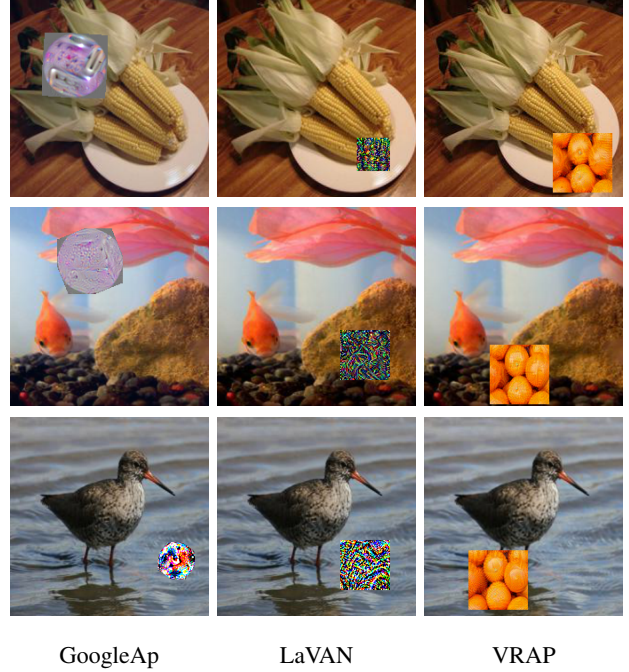


Figure 1. The adversarial patches w.r.t. the same input image generated by GoogleAp, LAVAN and our purposed VRAP, in which all the images are from ImageNet dataset.

As the research of adversarial examples progresses, various types of adversarial attacks have been proposed, such as adversarial patches [4, 24, 32], backdoor attacks [5, 31], weight-level attacks [2, 40]. Compared with adversarial examples, backdoor attacks, and weight-level attacks, adversarial patches can be printed to attack real-world applications, such as face recognition [44, 56, 59], autonomous driving [12, 38], making it become one of the most popular adversarial attacks [45]. Hence, it is essential to conduct an in-depth analysis of the intrinsic properties of adversarial patches.

Numerous works [4, 12, 32, 44] have been proposed to enhance the attack ability of adversarial patches. As shown in Fig. 1, however, we find that most adversarial patches are not as realistic as the real scrawls [4, 24], making it

easy to be detected when deployed in the physical world. Given the common existence of scrawls and logos, we can disguise the adversarial patches as scrawls to make them inconspicuous in the physical world. Thus, we argue that adversarial patches should be visually realistic instead of strange patterns to humans. To this end, we explore how to effectively and efficiently generate visually realistic adversarial patches.

In this work, we first analyze that a high-quality adversarial patch in the physical world should be 1) *realistic*: it would be similar to the real scrawls or logos; 2) *position irrelevant*: it would be easy to paste the patch to the real scenes; and 3) *printable*: it can be pasted to common scenes. Based on this analysis, we propose an effective visually realistic adversarial patch generating algorithm, called VRAP. In particular, VRAP constrains the adversarial patches in the ϵ -neighborhood of a real image to guarantee the visual reality; iteratively maximizes the loss at the position with the minimum loss in a local neighborhood of the current patch to ensure position irrelevant; smooths the patches using Total Variation loss and gamma transformation to make it printable. Our main contributions are summarized as follows:

- We analyze that a high-quality adversarial patch should be *realistic*, *position irrelevant* and *printable* to be deployed in the physical world.
- To the best of our knowledge, it is the first work that aims to generate realistic adversarial patches using any natural images for the image classification task.
- We propose a novel attack called VRAP to craft visually realistic adversarial patches by constraining the adversarial patches in the neighborhood of a real image. Despite the common belief that adversarial examples are not printable, the adversarial patches crafted by VRAP can be printed to attack DNNs in the physical world.
- Empirical evaluations on ImageNet dataset show its high effectiveness in the digital world and ability to naturally attack real-world applications without being detected.

2. Related Work

In this section, we provide a brief overview of the existing works about adversarial examples in the digital world and adversarial patches in the physical world.

Adversarial Examples in the Digital World. Szegedy et al. [46] first identified the vulnerability of DNNs to adversarial examples in the digital world, which are indistinguishable from benign ones by adding tiny perturbations but lead to incorrect predictions. Recently, numerous works have been proposed to generate more powerful adversarial examples, which mainly fall into two categories: 1) *White-box setting*: the attacker [9, 27, 36, 47, 50] can access any information of target model, *e.g.*, outputs, architecture, (hyper-)parameters, gradient, *etc.* 2) *Black-box set-*

ting: the attacker only allows access to limited information, which can be further split into three categories: a) *Score-based attacks* [7, 15, 22, 30] utilize the prediction probability to craft adversarial examples. b) *Decision-based attacks* [3, 6, 28, 53] can only access the prediction label for attack. c) *Transfer-based attacks* [10, 51, 52, 60] adopt the adversarial examples generated on the surrogate model to attack the target model. Adversarial examples perform very well in digital world [1, 48, 54], which could attack online commercial APIs taking digital images as input [28, 53], but the imperceptible perturbation makes it hard to be deployed in the physical world [4].

Adversarial Patches in the Physical World. Different from adversarial examples that add imperceptible perturbation to the image, adversarial patches paste a small but noticeable patch to the benign image to fool the target model, which can be printed in the physical world. Brown et al. [4] first proposed GoogleAp to generate a universal and printable adversarial patch to fool the classifier by maximizing the loss of a patch initialized by a real image patch on several images simultaneously. Currently, adversarial patches have become one of the primary forms of physical attacks [45]. LaVAN [24] shows that a small localized adversarial noise is enough to fool the classifier. PatchAttack [63] adopts reinforcement learning to optimize the adversarial texture patch from a designed texture dictionary. Several works adopt generative adversarial network (GAN) [13] to craft adversarial patches. PS-GAN [32] adopts a perceptual-sensitive generative adversarial network to improve visual fidelity. PEPG [62] fine-tunes a pretrained GAN to generate virtual insects as adversarial patches to fool the classifier. GDPA [29] employs a generator to generate dynamic/static patch patterns and locations for the given input image. Adversarial patches are also widely adopted in other domains, such as object detection [18, 19, 21, 61], face recognition [25, 44, 56, 59] and autonomous driving [11, 12, 38, 67]. To the best of our knowledge, however, except for a few adversarial patches using the real sticker to fool face recognition [56] or object detector [18], most adversarial patches are not *visually realistic* so that they are significantly different from real scrawls, making them easy to be detected in the physical world.

In this work, we argue that a high-quality adversarial patch should be *visually realistic* to make it inconspicuous in the physical world. Thus, we propose a novel adversarial attack, called VRAP, to efficiently and effectively generate adversarial patches for the image classification task.

3. Methodology

Here we first introduce preliminaries, and analyze the crucial properties of high-quality adversarial patches. Then we detail our VRAP.

3.1. Preliminaries

Given a classifier f with parameters θ and benign image $\mathbf{x} \in \mathbb{R}^{H \times W \times C}$ labeled $\mathbf{y} \in \mathbb{R}^N$, adversarial patch is defined as:

Definition 1 (*Adversarial Patch*). *Adversarial patch is an additive patch $\bar{\mathbf{x}} \in \mathbb{R}^{H \times W \times C}$ with a location mask $\mathbf{m} \in \{0, 1\}^{H \times W \times C}$ that satisfies:*

$$f(\tilde{\mathbf{x}}; \theta) \neq f(\mathbf{x}; \theta) = y, \text{ where } \tilde{\mathbf{x}} = (1 - \mathbf{m}) \odot \mathbf{x} + \mathbf{m} \odot \bar{\mathbf{x}},$$

where \odot is element-wise multiplication.

Suppose h and w are the height and width and (i, j) is the index of the upper left corner of the region of $1s$ in the location mask \mathbf{m} , $\delta \in \mathbb{R}^{h \times w \times C}$ is the corresponding additive patch of $\bar{\mathbf{x}}$, we can denote the crafted adversarial patches as:

$$\tilde{\mathbf{x}} = \mathbf{x} +_{i,j} \delta, \quad (1)$$

where $+_{i,j}$ indicates pasting the patch δ to \mathbf{x} at the position (i, j) . We will use such notation in the rest of the paper without ambiguity. To generate adversarial patch, we can regard the attack as an optimization problem that searches an image patch δ with the size (w, h, C) as well as the position (i, j) that maximizes the loss function J of the target classifier:

$$(\delta, i, j) = \underset{\substack{\delta \in \mathbb{R}^{w \times h \times C} \\ 0 \leq i \leq H-h, 0 \leq j \leq W-w}}{\operatorname{argmax}} J(\tilde{\mathbf{x}}, y; \theta), \quad (2)$$

where $\tilde{\mathbf{x}}$ is calculated by Eq. (1).

3.2. Crucial Properties of Adversarial Patch

Brown et al. [4] first proposed adversarial patch, which can be printed and added to any scene to deceive classifiers. Due to its good applicability to attack the DNNs in the physical world, it has gained increasing interests [12, 21, 32, 59, 61]. However, existing adversarial patches, even those initialized by real images [4], are often unrealistic to human perception, making them easily detectable in the physical world. Also, there are no consistent properties of adversarial patches among the existing works, for instance, whether it should be unrelated to single image [4, 24], whether it should lead the DNNs to target prediction [32, 63]. Here we first analyze what crucial properties a high-quality adversarial patch should have to be deployed in the physical world:

- *Realistic*: As noticed by previous works [32], there are often meaningful scrawls, logos or patterns on the objects in the physical world. To make the adversarial patches inconspicuous, they should be visually realistic so that humans mistakenly take them as such real scrawls.

- *Position irrelevant*: Since we need to add the patches to the scenes manually, it is hard to place the patches in a precise position. Hence, a high-quality adversarial patch should be related to its position so that it can be easy to be deployed in the physical world.
- *Printable*: Adversarial patches should work effectively in the digital world as well as the physical world. Thus, it must be printable to be pasted into physical objects.

We argue that the above properties are necessary to make adversarial patches inconspicuous in the physical world. Other significant properties are beyond our discussion. For instance, the patches are universal for various scenes [21] or the patches cover objects with arbitrary shapes [19]. In this work, we show that adding perturbation to any image patches can craft realistic adversarial patches and design a novel attack in the next section.

3.3. Crafting Visually Realistic Adversarial Patch

Based on the above analysis, visual reality is of utmost importance for a high-quality adversarial patch. PS-GAN [32] employs a perceptual-sensitive generative adversarial network to enhance the visual fidelity for traffic sign recognition tasks, but the crafted adversarial patches are still not as realistic as real scrawls. Wei et al. [56] manipulate the actual sticker’s position and rotation angle on the objects for face recognition. However, precise positioning and angle adjustments can pose deployment challenges in the physical world. Hu et al. [18] sample the optimal image patch from a pretrained generative adversarial network for a high-quality adversarial patch against an object detector. However, these patches tend to be large, almost covering half of a T-shirt, which may not be ideal for practical applications. In this work, we first explore that:

How can we guarantee the visual reality of adversarial patches while maintaining high attack performance?

Note that adversarial examples are visually realistic as they add tiny perturbations to the benign samples to make them imperceptible [46]. This inspires us that constraining the image patches in the ϵ -neighborhood of benign samples can ensure the visual reality. Thus, we first investigate whether pasting such image patches to benign images on a fixed position can fool the target model:

$$\delta = \underset{\delta \in \mathbb{B}_\epsilon(\bar{\mathbf{x}})}{\operatorname{argmax}} J(\mathbf{x} +_{i,j} \delta, y; \theta), \quad (3)$$

where (i, j) is a fixed position, $\bar{\mathbf{x}}$ is the benign image patch with the size of (w, h, C) and $\mathbb{B}_\epsilon(\bar{\mathbf{x}}) = \{\mathbf{x}' : \|\mathbf{x}' - \bar{\mathbf{x}}\| \leq \epsilon\}$. Inspired by PGD optimization procedure [34], we solve Eq. (3) iteratively as follows:

$$\delta_{t+1} = \Pi_{\mathbb{B}_\epsilon(\bar{\mathbf{x}})}[\delta_t + \alpha \cdot \operatorname{sign}(\nabla_{\delta_t} J(\mathbf{x} +_{i,j} \delta_t, y; \theta))],$$

where $\delta_0 = \bar{\mathbf{x}}$, $\nabla_{\delta} J(\mathbf{x} +_{i,j} \delta, y; \theta)$ is the gradient of loss function w.r.t. δ , $\Pi_{\mathbb{B}_\epsilon(\bar{\mathbf{x}})}(\cdot)$ projects the input into $\mathbb{B}_\epsilon(\bar{\mathbf{x}})$ and $\operatorname{sign}(\cdot)$ denotes the sign function.

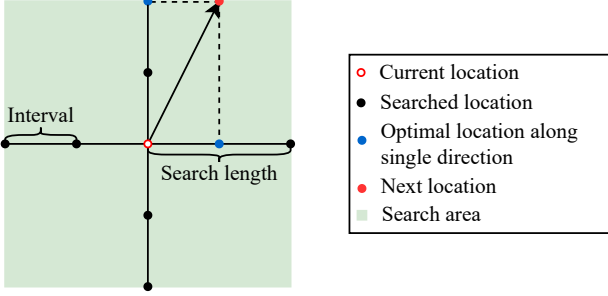


Figure 2. An illustration of local search for the next position.

We conduct the above attack in a randomly fixed position (i, j) on VGG-16 model in the digital world with different perturbation budget ϵ . As shown in the Appendix, we can successfully generate visually realistic adversarial patches in the neighborhood of the benign image patches with high attack performance. However, it is well-known that the imperceptible adversarial perturbations are too hard for printing to be deployed in the physical world. This brings us another issue:

How can we make such visually realistic adversarial patches printable?

To address this issue, we analyze what information will be lost when printing the image. 1) The range of colors that printers can reproduce is a subset of RGB space, *i.e.*, the printer introduces a small deviation to the brightness (RGB colors in the digital world). Thus, adversarial patches should not be sensitive to such deviations. To mitigate this effect, we use gamma correction to ensure that the poorest patch in the neighborhood of the current patch can fool the target model:

$$G(\delta, \lambda, \gamma) = \lambda \cdot \delta^\gamma,$$

where λ and γ are the learnable parameters in this work. 2) Due to the limited range of colors, the contrast of image would decrease so that the printed image might lose some local details. Therefore, the colors in the generated adversarial patches should change gradually like natural images. To maintain the smoothness of perturbation, we add the total variation loss as a regularizer:

$$\mathcal{L}_{TV}(\delta) = \sum_{i,j} |\delta_{i,j+1} - \delta_{i,j}| + |\delta_{i+1,j} - \delta_{i,j}|.$$

To generate the printable adversarial patches, Eq. (3) is rewritten as:

$$\delta = \underset{\delta \in \mathbb{B}_\epsilon(\bar{x})}{\operatorname{argmax}} \min_{\lambda, \gamma} J(\mathbf{x} +_{i,j} G(\delta, \lambda, \gamma), y; \theta) + \mathcal{L}_{TV}(\delta).$$

The position irrelevance means that the generated adversarial patch pasted to various positions of the given image can successfully fool the target model. However, directly

Algorithm 1 VRAP

Input: A classifier f with the parameters θ and loss function J ; a raw example x with the ground-truth label y , and the initial real image patch \bar{x} ; the perturbation budget ϵ ; the number of iteration T ; search range k and stepsize τ

Output: An adversarial patch δ

- 1: $\alpha = \epsilon/T, \beta = \epsilon/T, g_0 = 0, \delta_0 = \hat{x}, \lambda = 1, \gamma = 1$
- 2: Randomly sample the position (i, j)
- 3: **for** $t = 0 \rightarrow T - 1$ **do**
- 4: update position (i, j) by optimizing Eq. (4) using local search
- 5: Calculate the gradient w.r.t. δ :

$$g_t = \nabla_\delta [J(\mathbf{x} +_{i,j} G(\delta_t, \lambda, \gamma), y; \theta) + L_{TV}(\delta_t)]$$

- 6: Update the adversarial patch δ_t :

$$\delta_{t+1} = \Pi_{\mathbb{B}_\epsilon(\bar{x})}[\delta_t + \alpha \cdot \operatorname{sign}(g_t)]$$

- 7: Calculate the gradient w.r.t. λ and γ :

$$g_\lambda, g_\gamma = \nabla_{\lambda, \gamma} [J(\mathbf{x} +_{i,j} G(\delta_{t+1}, \lambda, \gamma), y; \theta) + L_{TV}(\delta_{t+1})]$$

- 8: Update λ and γ using gradient descent:

$$\lambda = \lambda - \beta \cdot g_\lambda, \quad \gamma = \gamma - \beta \cdot g_\gamma$$

- 9: **end for**

- 10: **return** δ_T
-

optimizing the position is an integer programming problem, which is NP-complete. With numerous potential positions in the given image, we adopt local search to find the poorest position around the current position, *i.e.*, the position (i^*, j^*) in the neighborhood of position (i, j) that minimizes the loss:

$$(i^*, j^*) = \underset{\substack{i-k \leq i' \leq i+k, \\ j-k \leq j' \leq j+k}}{\operatorname{argmin}} J(\mathbf{x} +_{i',j'} \delta, y; \theta), \quad (4)$$

where k is the search range. Since each query needs forward propagation, the grid search still takes a large number of queries, resulting in a huge computation cost. As shown in Fig. 2, we search the position along x-axis and y-axis to find the optimal position (i^*, j) and (i, j^*) . Then we approximately combine the best positions in these directions as the optimal position (i^*, j^*) . Since shifting the patch within a few pixels does not bring obvious distinction, we search the positions with a stepsize τ to further boost the efficiency. In summary, the objective function can be for-

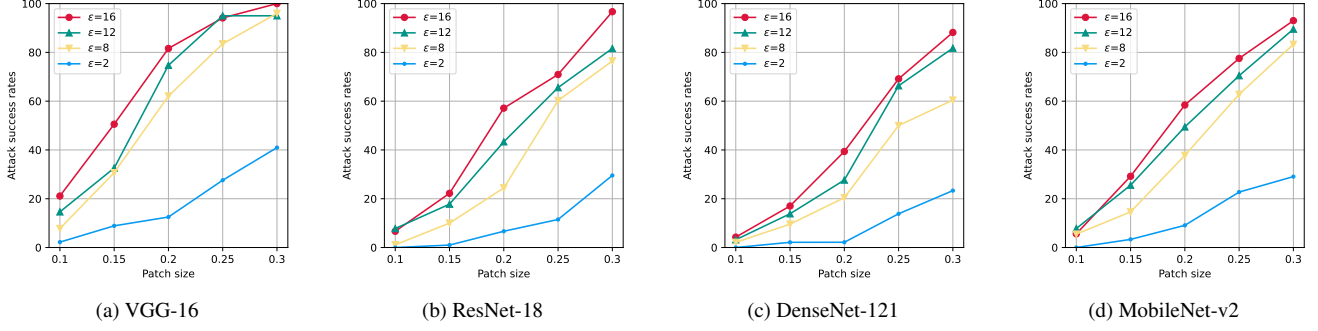


Figure 3. Attack success rates (%) of VRAP on four models with various perturbation budgets and patch sizes.

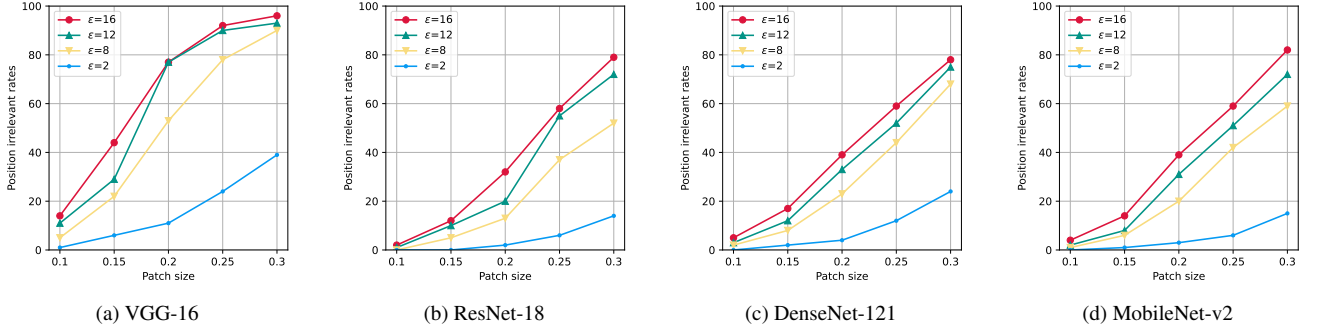


Figure 4. Position irrelevant rates (%) of VRAP on four models with various perturbation budgets and patch sizes.

mulated as:

$$\delta = \underset{\delta \in \mathbb{B}_\epsilon(\bar{\mathbf{x}})}{\operatorname{argmax}} \min_{\substack{\lambda, \gamma, \\ 0 \leq i \leq H-h, \\ 0 \leq j \leq W-w}} J(\mathbf{x} + i, j G(\delta, \lambda, \gamma), y; \theta) + \mathcal{L}_{TV}(\delta),$$

in which $\bar{\mathbf{x}}$ is any benign image with the size of (h, w, C) . The algorithm of the proposed Visually Realistic Adversarial Patch attack (VRAP) is summarized in Algorithm 1.

4. Experiments

In this section, we evaluate the visually realistic adversarial patches in the digital as well as physical world, and explore why these realistic patches can effectively attack DNNs.

4.1. Experimental Setting

We summarize our experimental setting as follows:

Dataset. We use 1,000 images pertaining to 1,000 classes from ILSVRC 2012 validation set [39], which are almost correctly classified by the chosen deep models.

Models. We utilize several popular deep models with different architectures for image classification, including VGG-16 [23], ResNet-18 [17], DenseNet-121 [20], MobileNet-v2 [35]. All the classifiers are trained on ImageNet and achieve a classification accuracy of 90.4%, 93.4%, 90.2%, and 95.3% on our evaluation dataset. We also study several adversarial patch defense models, including DW [16], and LGS [37], PatchGuard [58], CBN [66],

and several methods against adversarial examples, *i.e.*, Random Smoothing [8] and FastAT [57].

Evaluation Metrics. We mainly evaluate the attack success rate of VRAP, the portion of images with the adversarial patches can mislead the target model but the images with original patches can be correctly classified. Given an image set \mathcal{X} , we can formulate the attack success rate (ASR) as:

$$\text{ASR}(\mathcal{X}) = \frac{1}{|\mathcal{X}|} \sum_{x \in \mathcal{X}} \mathbb{I}(f(x + i, j \delta) \neq y) \cdot \mathbb{I}(f(x + i, j \delta_0) = y),$$

where $\mathbb{I}(\cdot)$ is the indicator function, δ is the adversarial patch and δ_0 is the original patch. To evaluate the position irrelevant performance, we also define the position irrelevant rates (PIR) for a give image x as:

$$\text{PIR}(x) = \frac{\sum_{\substack{0 \leq \tau \cdot i \leq H-h \\ 0 \leq \tau \cdot j \leq W-w}} \mathbb{I}(f(x + \tau \cdot i, \tau \cdot j \delta) \neq y))}{\lfloor (H-h)/\tau \rfloor \lfloor (W-w)/\tau \rfloor},$$

where τ is the step size, (H, W) and (h, w) are the size of the input image x and the adversarial patch, respectively.

Hyper-parameters. We adopt the search range of 10 with stepsize of 5 to conduct the main evaluations.

4.2. Evaluation on Attacking Ability

To validate the effectiveness of VRAP, we evaluate the attack success rates and position irrelevant rates of adversarial

patches with various patch sizes and perturbation budgets on four widely adopted deep models. We also visualize the adversarial patches in the Appendix. The patch size is the relative size of the patch compared with the input image.

Attack success rates. The attack success rates on four deep models are summarized in Fig. 3. In general, increasing the patch size can consistently improve the attack success rates on all four models, since the patch occupies a larger proportion in the original image. Besides, the perturbation budget constrains the search space for the adversarial patch. As expected, we can observe that the larger perturbation budget results in better attack success rates with the same patch size. In particular, when the patch size is 0.3 with the perturbation budget $\epsilon = 16$, the attack success rates are larger than 90.0% on four models. Besides, on VGG-16 with the patch size of 0.3, VRAP can achieve 100.0% attack success rate with $\epsilon = 16$ and more than 95% when the perturbation budget $\epsilon \geq 8$. Such high and stable attack performance on the four deep models shows the remarkable effectiveness of VRAP to generate visually realistic adversarial patches.

Position irrelevant rates. Since we need to paste the adversarial patch to real-world objects manually, it is hard to place them in a precise position, making it crucial for the patch to be position irrelevant. To verify such property of adversarial patches crafted by VRAP, we calculate the position irrelevant rates on four models and summarize the results in Fig. 4. Note that we adopt a brute force algorithm to calculate the position irrelevant rates, in which a $224 \times 224 \times 3$ image and an adversarial patch with the patch size of 0.3 take thousands of predictions using the interval $\tau = 5$. Due to such colossal computation cost, we adopt 100 images for evaluation. Similar to the attack success rates, a larger patch size or perturbation budget also boosts the position irrelevant rates. In most cases, VRAP can achieve the position irrelevant rate of more than 40.0% on all four models. Specifically, with the patch size of 0.3 and perturbation budget $\epsilon = 16$, VRAP achieves the position irrelevant rate near 100.0% on VGG-16 and around 80.0% on the other three models. Such superior performance makes VRAP easy to be deployed in the physical world without careful placement.

4.3. Evaluation on Defense Method

Here we evaluate the effectiveness of VRAP against several adversarial patch defense methods including DW, LGS, PatchGuard, and CBN. For DW and LGS, we craft the adversarial patch of size 0.3 and $\epsilon = 16$ with VGG-16. For PatchGuard and CBN, we follow their experiment setting in their papers and craft the adversaries on BagNet-17 to evaluate our proposed methods. To further validate the effectiveness of VRAP, we also consider two adversarial defense methods, *i.e.*, RS and FastAT.



Figure 5. The raw images, images with original image patches, and adversarial patches in the physical world. See more samples in Appendix.

The attack performance is summarized in Tab 1. VRAP can pass adversarial patch defense methods with a high average attack success rate of 83.4%, and a high position irrelevant rate of 78.9%. It validates that our VRAP can bypass adversarial patch mechanisms. For certified and adversarial training methods, VRAP exhibitS weaker performance, the average attack success rate and position irrelevant rate against several defense methods is 65.2% and 58.9% respectively. It further validates the effectiveness of VRAP.

4.4. Evaluation in Physical World

The main advantage of adversarial patches is to be deployed in the physical world. VRAP makes it easier to place the adversarial patches and harder to be detected. Here we adopt ResNet-18 as the target model to conduct the evaluation in the physical world. We first take a photo of the real-world object, which can be correctly classified. Then we generate an adversarial patch using VRAP and print it by HITI digital photo printer P910L. Finally, we put the printed adversarial patch around the object and take a photo for recognition.

Metric	LGS	DW	PatchGuard	CBN	DRS	Avg.
ASR (%)	94.9	92.2	80.8	65.6	33.3	73.4
PIR (%)	89.8	90.1	73.5	62.2	23.5	61.8

Table 1. Attack success rates (%) and position irrelevant rates (%) of five defense methods.

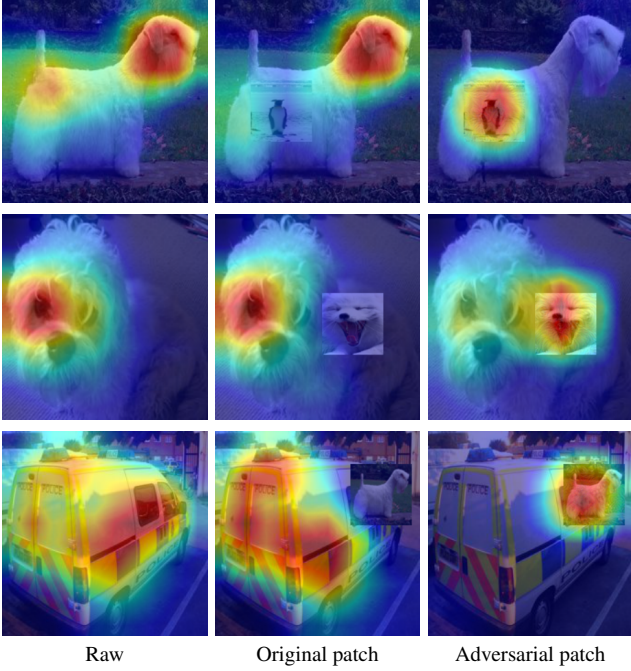


Figure 6. Attention heatmaps of raw image, the image with original patch and adversarial patches on ResNet-18. See more samples in the Appendix.

As shown in Fig. 5a, we choose three everyday things in life, namely water bottle, toilet paper and mouse, which can be correctly classified. After placing the original image patch on the corresponding object illustrated in Fig. 5b, the model can still make the correct prediction, supporting that the deep models are robust to such a natural image patch. From Fig. 5c, we can observe that there is no visual difference between the original patch and the adversarial patch in the physical world, which guarantees the visual reality of adversarial patches. When we put the adversarial patches in the same position of the original patch in Fig. 5b, the images with adversarial patches can successfully fool the victim model. Due to the reality of adversarial patches, they can easily disguise as logos or scrawls on the objects, making it hard to distinguish these adversarial patches and natural ones. Such superior visual reality and ease of deployment in various scenes support that VRAP can be widely used to attack real-world applications without being detected. The reality also makes the attack imperceptible, which reveals a new and significant threat to commercial applications.

4.5. Discussion

Based on the above evaluations, we can conclude that VRAP can generate visually realistic adversarial patches in both digital and physical worlds to fool the deep models, which are hard for humans to perceive. As the first attack that focuses on generating visually realistic adversarial patches, we empirically investigate why such visually realistic patches can successfully fool the victim models. Since the deep models are not explainable, we adopt Grad-CAM, a widely adopted approach to calculate the attention heatmaps on the input image to highlight the significant features for recognition and interpret the model behavior on these images.

The attention heatmaps on the raw image, the image with the original patch and the adversarial patch at a random position are reported in Fig. 6. As we can see, adding the original patch to the image does not change the attention heatmaps and cannot mislead the deep models, showing the stability and robustness of the model on these naturally transformed images. However, the attention heatmaps of the images with the adversarial patches are mainly located in the part of the added patch, which is significantly different from that on the original images. Hence, different from adversarial perturbation that makes the target model predict incorrectly, the perturbation in our adversarial patch misleads the victim model to focus on the wrong area. Without extracting the correct feature of the input image, the deep model cannot make the correct prediction. Interestingly, we also find that the prediction on these images is not consistent with the ground-truth label of the original patch, though the attention heatmaps are mainly on the patch. The reasons might be twofold: 1) The perturbation on the patch might also mislead the victim model, which is similar to adversarial perturbation. 2) The patch only occupies a small area of the image so that its surrounding image makes it hard for the deep model to recognize the patch. We will conduct more exploration and theoretical analysis to under why the visually realistic adversarial patches mislead the deep models in our future work.

4.6. Parameter Studies

We conduct a series of experiments to study the impact of two hyper-parameters to find the poorest position for optimizing the perturbation, namely the search interval and search range.

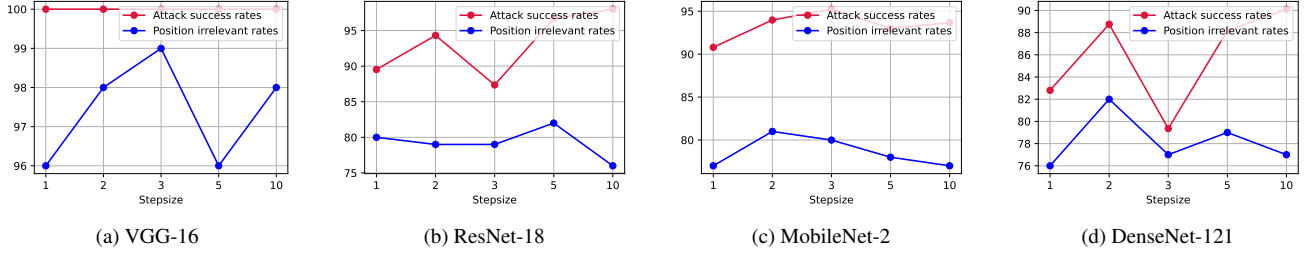


Figure 7. Attack successful rates (%) and position irrelevant rates (%) of various models using VRAP on various stepsizes with the default search range $k = 10$.

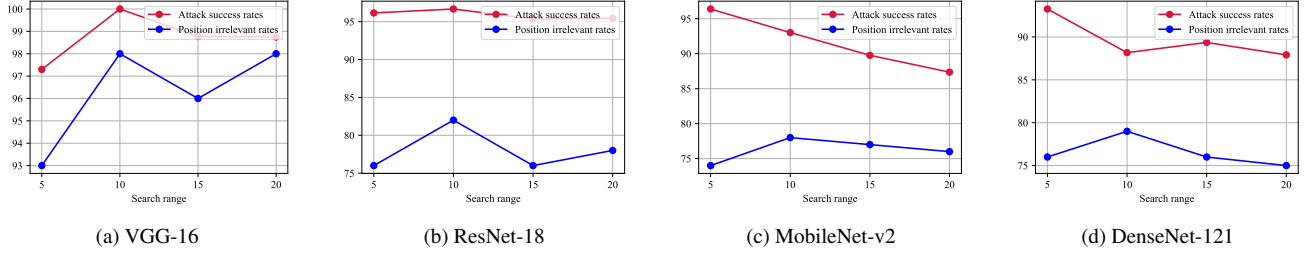


Figure 8. Attack successful rates (%) and position irrelevant rates (%) of various models using VRAP on various search ranges with the default stepsize $\tau = 5$.

On the stepsize τ . The stepsize τ helps VRAP ignore several positions along the axis to boost the efficiency. We first investigate whether a large stepsize degrades the attack performance without checking each possible position. Specifically, we implement VRAP with various stepsizes on all four models and report the attack success rates and position irrelevant rates in Fig. 7. As we can see, when we adopt different stepsizes, the attack success rates and position irrelevant rates fluctuate in an acceptable range on all four models. This indicates that a large stepsize does not significantly decrease the attack performance but accelerates the search process. To balance the attack efficiency and effectiveness, we simply set $\tau = 5$ in our experiments.

On the search range k . The search range k constrains the size of the neighborhood to find a better position using local search. VRAP cannot find a suitable position with a small search range k , since it cannot effectively explore the neighborhood. With a large neighborhood, the approximation introduces a larger error when estimating the best position, which will also degrade the performance. To find a suitable search range k , we adopt various k to conduct experiments on all four models. As shown in Fig. 8, when $k = 5$, VRAP achieves the lowest position irrelevant rates. When we increase k , the position irrelevant rates increase first but decrease slightly after $k > 10$. Besides, the attack success rates are not significantly affected by various search ranges on these models. Hence, we adopt $k = 10$ in our experiments.

In summary, the stepsize τ accelerates the local search without decreasing the attack performance, while a suitable search range results in better position irrelevant rates. In our experiments, we adopt $\tau = 5$ and $k = 10$ for better efficiency and effectiveness.

5. Conclusion

In this work, we first analyze and conclude that a high-quality adversarial patch should be *realistic*, *position irrelevant*, and *printable* to be effectively deployed in the physical world. Based on this analysis, we propose the first visually realistic adversarial patch generating algorithm, denoted as VRAP. Specifically, VRAP iteratively optimizes the perturbation based on the real patch using a Total Variation loss and gamma transformation in the searched position with the minimum loss. Extensive evaluations on ImageNet dataset demonstrate that VRAP exhibits superior attack success rates and position irrelevant rates on various deep models in the digital world. Since the generated patches are realistic, position irrelevant, and printable, it is easy to deploy them in the physical world to fool deep models which are hard for humans to detect, raising a significant threat to DNNs-enabled applications. We hope our work can provide insights to generate these visually realistic patches for real-world attack, and draw more attention to mitigating the threat of such adversarial patches.

References

- [1] Anish Athalye, Nicholas Carlini, and David Wagner. Obfuscated Gradients Give a False Sense of Security: Circumventing Defenses to Adversarial Examples. pages 274–283, 2018. 2
- [2] Jakub Breier, Xiaolu Hou, Dirmanto Jap, Lei Ma, Shivam Bhasin, and Yang Liu. DeepLaser: Practical Fault Attack on Deep Neural Networks. In *Proceedings of the ACM SIGSAC Conference on Computer and Communications Security*, pages 2204–2206, 2018. 1
- [3] Wieland Brendel, Jonas Rauber, and Matthias Bethge. Decision-Based Adversarial Attacks: Reliable Attacks Against Black-Box Machine Learning Models. *International Conference on Learning Representations*, 2018. 2
- [4] Tom B. Brown, Dandelion Mané, Aurko Roy, Martín Abadi, and Justin Gilmer. Adversarial Patch. In *Neural Information Processing Systems (Workshop)*, 2017. 1, 2, 3
- [5] Xinyun Chen, Chang Liu, Bo Li, Kimberly Lu, and Dawn Song. Targeted Backdoor Attacks on Deep Learning Systems Using Data Poisoning. In *arXiv preprint arXiv:1712.05526*, 2017. 1
- [6] Minhao Cheng, Thong Le, Pin-Yu Chen, Huan Zhang, Jinfeng Yi, and Cho-Jui Hsieh. Query-Efficient Hard-label Black-box Attack: An Optimization-based Approach. In *International Conference on Learning Representations*, 2019. 2
- [7] Shuyu Cheng, Yinpeng Dong, Tianyu Pang, Hang Su, and Jun Zhu. Improving black-box adversarial attacks with a transfer-based prior. In *Advances in Neural Information Processing Systems*, pages 10932–10942, 2019. 2
- [8] Jeremy M Cohen, Elan Rosenfeld, and J Zico Kolter. Certified adversarial robustness via randomized smoothing. In *International Conference on Machine Learning*, 2019. 5
- [9] Francesco Croce and Matthias Hein. Reliable Evaluation of Adversarial Robustness with an Ensemble of Diverse Parameter-free Attacks. In *International conference on machine learning*, pages 2206–2216, 2020. 2
- [10] Yinpeng Dong, Fangzhou Liao, Tianyu Pang, Hang Su, Jun Zhu, Xiaolin Hu, and Jianguo Li. Boosting Adversarial Attacks with Momentum. In *Proceedings of the IEEE Conference on Computer Vision and Pattern Recognition*, pages 9185–9193, 2018. 1, 2
- [11] Ranjie Duan, Xingjun Ma, Yisen Wang, James Bailey, A Kai Qin, and Yun Yang. Adversarial Camouflage: Hiding Physical-World Attacks With Natural Styles. In *Proceedings of the IEEE/CVF conference on computer vision and pattern recognition*, pages 1000–1008, 2020. 2
- [12] Kevin Eykholt, Ivan Evtimov, Earlene Fernandes, Bo Li, Amir Rahmati, Chaowei Xiao, Atul Prakash, Tadayoshi Kohno, and Dawn Song. Robust Physical-World Attacks on Deep Learning Visual Classification. In *Proceedings of the IEEE Conference on Computer Vision and Pattern Recognition*, pages 1625–1634, 2018. 1, 2, 3
- [13] Ian Goodfellow, Jean Pouget-Abadie, Mehdi Mirza, Bing Xu, David Warde-Farley, Sherjil Ozair, Aaron Courville, and Yoshua Bengio. Generative Adversarial Nets. In *Advances in Neural Information Processing Systems*, pages 2672–2680, 2014. 2
- [14] Ian J Goodfellow, Jonathon Shlens, and Christian Szegedy. Explaining and harnessing adversarial examples. In *International Conference on Learning Representations*, 2015. 1
- [15] Chuan Guo, Jacob Gardner, Yurong You, Andrew Gordon Wilson, and Kilian Weinberger. Simple Black-box Adversarial Attacks. In *International Conference on Machine Learning*, pages 2484–2493, 2019. 2
- [16] Jamie Hayes. On Visible Adversarial Perturbations & Digital Watermarking. In *Proceedings of the IEEE Conference on Computer Vision and Pattern Recognition (Workshop)*, pages 1597–1604, 2018. 5
- [17] Kaiming He, Xiangyu Zhang, Shaoqing Ren, and Jian Sun. Deep Residual Learning for Image Recognition. In *Proceedings of the IEEE Conference on Computer Vision and Pattern Recognition*, pages 770–778, 2016. 1, 5
- [18] Yu-Chih-Tuan Hu, Bo-Han Kung, Daniel Stanley Tan, Jun-Cheng Chen, Kai-Lung Hua, and Wen-Huang Cheng. Naturalistic Physical Adversarial Patch for Object Detectors. In *Proceedings of the IEEE/CVF International Conference on Computer Vision*, pages 7848–7857, 2021. 2, 3
- [19] Zhanhao Hu, Siyuan Huang, Xiaopei Zhu, Fuchun Sun, Bo Zhang, and Xiaolin Hu. Adversarial Texture for Fooling Person Detectors in the Physical World. In *Proceedings of the IEEE/CVF Conference on Computer Vision and Pattern Recognition*, pages 13307–13316, 2022. 2, 3
- [20] Gao Huang, Zhuang Liu, Laurens Van Der Maaten, and Kilian Q Weinberger. Densely connected convolutional networks. In *Proceedings of the IEEE Conference on Computer Vision and Pattern Recognition*, pages 4700–4708, 2017. 5
- [21] Lifeng Huang, Chengying Gao, Yuyin Zhou, Cihang Xie, Alan L Yuille, Changqing Zou, and Ning Liu. Universal Physical Camouflage Attacks on Object Detectors. In *Proceedings of the IEEE Conference on Computer Vision and Pattern Recognition*, pages 720–729, 2020. 2, 3
- [22] Andrew Ilyas, Logan Engstrom, Anish Athalye, and Jessy Lin. Black-box Adversarial Attacks with Limited Queries and Information. In *International Conference on Machine Learning*, pages 2142–2151, 2018. 2
- [23] Simonyan Karen and Zisserman Andrew. Very Deep Convolutional Networks for Large-Scale Image Recognition. In *International Conference on Learning Representations*, 2015. 5
- [24] Danny Karmon, Daniel Zoran, and Yoav Goldberg. LaVAN: Localized and Visible Adversarial Noise. In *International Conference on Machine Learning*, 2018. 1, 2, 3
- [25] Stepan Komkov and Aleksandr Petiushko. AdvHat: Real-world adversarial attack on ArcFace Face ID system. In *International Conference on Pattern Recognition*, pages 819–826, 2021. 2
- [26] Alex Krizhevsky, Ilya Sutskever, and Geoffrey E. Hinton. ImageNet Classification with Deep Convolutional Neural Networks. In *Neural Information Processing Systems*, pages 1106–1114, 2012. 1
- [27] Alexey Kurakin, Ian Goodfellow, and Samy Bengio. Adversarial Examples in the Physical World. In *International*

- Conference on Learning Representations (Workshop)*, 2017. 2
- [28] Huichen Li, Xiaojun Xu, Xiaolu Zhang, Shuang Yang, and Bo Li. QEBA: Query-Efficient Boundary-Based Blackbox Attack. In *Proceedings of the IEEE Conference on Computer Vision and Pattern Recognition*, pages 1218–1227, 2020. 2
- [29] Xiang Li and Shihao Ji. Generative Dynamic Patch Attack. 2021. 2
- [30] Yandong Li, Lijun Li, Liqiang Wang, Tong Zhang, and Boqing Gong. N ATTACK: Learning the Distributions of Adversarial Examples for an Improved Black-Box Attack on Deep Neural Networks. In *International Conference on Machine Learning*, pages 3866–3876, 2019. 2
- [31] Yiming Li, Yong Jiang, Zhifeng Li, and Shutao Xia. Backdoor Learning: A Survey. In *IEEE Transactions on Neural Networks and Learning Systems*, 2022. 1
- [32] Aishan Liu, Xianglong Liu, Jiaxin Fan, Yuqing Ma, Anlan Zhang, Huiyuan Xie, and Dacheng Tao. Perceptual-Sensitive GAN for Generating Adversarial Patches. In *Proceedings of the AAAI Conference on Artificial Intelligence*, 2019. 1, 2, 3
- [33] Jonathan Long, Evan Shelhamer, and Trevor Darrell. Fully Convolutional Networks for Semantic Segmentation. In *Proceedings of the IEEE Conference on Computer Vision and Pattern Recognition*, pages 3431–3440, 2015. 1
- [34] Aleksander Madry, Aleksandar Makelov, Ludwig Schmidt, Dimitris Tsipras, and Adrian Vladu. Towards Deep Learning Models Resistant to Adversarial Attacks. In *International Conference on Learning Representations*, 2018. 3
- [35] Sandler Mark, Howard Andrew, Zhu Menglong, Zhmoginov Andrey, and Chen Liang-Chieh. Mobilenetv2: Inverted residuals and linear bottlenecks. In *Proceedings of the IEEE Conference on Computer Vision and Pattern Recognition*, page 4510–4520, 2018. 5
- [36] Seyed-Mohsen Moosavi-Dezfooli, Alhussein Fawzi, and Pascal Frossard. Deepfool: A Simple and Accurate Method to Fool Deep Neural Networks. In *Proceedings of the IEEE/CVF Conference on Computer Vision and Pattern Recognition*, pages 2574–2582, 2016. 2
- [37] Muzammal Naseer, Salman H. Khan, and Fatih Porikli. Local Gradients Smoothing: Defense against localized adversarial attacks. In *WACV. IEEE*, pages 1300–1307, 2019. 5
- [38] Federico Nesti, Giulio Rossolini, Saasha Nair, Alessandro Biondi, and Giorgio Buttazzo. Evaluating the Robustness of Semantic Segmentation for Autonomous Driving against Real-World Adversarial Patch Attacks. In *Proceedings of the IEEE/CVF Winter Conference on Applications of Computer Vision*, pages 2280–2289, 2022. 1, 2
- [39] Russakovsky Olga, Deng Jia, Su Hao, Krause Jonathan, Satheesh Sanjeev, Ma Sean, hUANG Zhiheng, Karpathy Andrej, Khosla Aditya, and et al Bernstein Michael. Imagenet large scale visual recognition challenge. In *International journal of computer vision*, pages 211–252, 2015. 5
- [40] Adnan Siraj Rakin, Zhezhi He, and Deliang Fan. TBT: Targeted Neural Network Attack With Bit Trojan. In *Proceedings of the IEEE/CVF Conference on Computer Vision and Pattern Recognition*, pages 13198–13207, 2020. 1
- [41] Joseph Redmon, Santosh Divvala, Ross Girshick, and Ali Farhadi. You Only Look Once: Unified, Real-Time Object Detection. In *Proceedings of the IEEE Conference on Computer Vision and Pattern Recognition*, pages 779–788, 2016. 1
- [42] Shaoqing Ren, Kaiming He, Ross Girshick, and Jian Sun. Faster R-CNN: Towards Real-Time Object Detection with Region Proposal Networks. In *Neural Information Processing Systems*, pages 91–99, 2015. 1
- [43] Olaf Ronneberger, Philipp Fischer, and Thomas Brox. U-Net: Convolutional Networks for Biomedical Image Segmentation. In *Medical Image Computing and Computer-Assisted Intervention*, pages 234–241, 2015. 1
- [44] Mahmood Sharif, Sruti Bhagavatula, Lujo Bauer, and Michael K. Reiter. Accessorize to a Crime: Real and Stealthy Attacks on State-of-the-Art Face Recognition. In *Proceedings of the ACM SIGSAC Conference on Computer and Communications Security*, pages 1528–1540, 2016. 1, 2
- [45] Abhijith Sharma, Yijun Bian, Phil Munz, and Apurva Narayan. Adversarial Patch Attacks and Defences in Vision-Based Tasks: A Survey. In *arXiv preprint arXiv:2206.08304*, 2022. 1, 2
- [46] Christian Szegedy, Wojciech Zaremba, Ilya Sutskever, Joan Bruna, Dumitru Erhan, Ian Goodfellow, and Rob Fergus. Intriguing properties of neural networks. In *International Conference on Learning Representations*, 2014. 1, 2, 3
- [47] Florian Tramèr, Alexey Kurakin, Nicolas Papernot, Ian Goodfellow, Dan Boneh, and Patrick McDaniel. Ensemble Adversarial Training: Attacks and Defenses. *International Conference on Learning Representations*, 2018. 2
- [48] Kunyu Wang, Xuanran He, Wenxuan Wang, and Xiaosen Wang. Boosting Adversarial Transferability by Block Shuffle and Rotation. *arXiv preprint arXiv:2308.10299*, 2023. 2
- [49] Xiaosen Wang and Kun He. Enhancing the transferability of adversarial attacks through variance tuning. In *Proceedings of the IEEE Conference on Computer Vision and Pattern Recognition*, 2021. 1
- [50] Xiaosen Wang, Kun He, Chuanbiao Song, Liwei Wang, and John E. Hopcroft. AT-GAN: A Generative Attack Model for Adversarial Transferring on Generative Adversarial Nets. *arXiv preprint arXiv:1904.07793*, 2019. 2
- [51] Xiaosen Wang, Xuanran He, Jingdong Wang, and Kun He. Admix: Enhancing the transferability of adversarial attacks. In *International Conference on Computer Vision*, pages 16138–16147, 2021. 2
- [52] Xiaosen Wang, Jiadong Lin, Han Hu, Jingdong Wang, and Kun He. Boosting Adversarial Transferability through Enhanced Momentum. In *British Machine Vision Conference*, 2021. 2
- [53] Xiaosen Wang, Zeliang Zhang, Kangheng Tong, Dihong Gong, Kun He, Zhifeng Li, and Wei Liu. Triangle Attack: A Query-efficient Decision-based Adversarial Attack. In *European conference on computer vision*, 2022. 2
- [54] Xiaosen Wang, Kangheng Tong, and Kun He. Rethinking the Backward Propagation for Adversarial Transferability. In *Proceedings of the Advances in Neural Information Processing Systems*, 2023. 2
- [55] Xiaosen Wang, Zeliang Zhang, and Jianping Zhang. Structure Invariant Transformation for better Adversarial Trans-

- ferability. In *Proceedings of the IEEE/CVF International Conference on Computer Vision*, pages 4607–4619, 2023. 1
- [56] Xingxing Wei, Ying Guo, and Jie Yu. Adversarial Sticker: A Stealthy Attack Method in the Physical World. In *IEEE Transactions on Pattern Analysis and Machine Intelligence*, 2022. 1, 2, 3
- [57] Eric Wong, Leslie Rice, and J.Zico Kolter. Fast is better than free: Revisiting adversarial training. In *International Conference on Learning Representations*, 2020. 5
- [58] Chong Xiang, Arjun Nitin Bhagoji, Vikash Sehwal, and Prateek Mittal. Patchguard: A provably robust defense against adversarial patches via small receptive fields and masking. In *30th USENIX Security Symposium (USENIX Security)*, 2021. 5
- [59] Zihao Xiao, Xianfeng Gao, Chilin Fu, Yinpeng Dong, Wei Gao, Xiaolu Zhang, Jun Zhou, and Jun Zhu. Improving Transferability of Adversarial Patches on Face Recognition with Generative Models. In *Proceedings of the IEEE Conference on Computer Vision and Pattern Recognition*, pages 11845–11854, 2021. 1, 2, 3
- [60] Cihang Xie, Zhishuai Zhang, Yuyin Zhou, Song Bai, Jianyu Wang, Zhou Ren, and Alan L Yuille. Improving Transferability of Adversarial Examples with Input Diversity. In *Proceedings of the IEEE Conference on Computer Vision and Pattern Recognition*, pages 2730–2739, 2019. 2
- [61] Kaidi Xu, Gaoyuan Zhang, Sijia Liu, Quanfu Fan, Mengshu Sun, Hongge Chen, Pin-Yu Chen, Yanzhi Wang, and Xue Lin. Adversarial T-shirt! Evading Person Detectors in A Physical World. In *European conference on computer vision*, pages 665–681, 2020. 2, 3
- [62] Hiromu Yakura, Youhei Akimoto, and Jun Sakuma. Generate (non-software) Bugs to Fool Classifiers. In *Proceedings of the AAAI Conference on Artificial Intelligence*, pages 1070–1078, 2020. 2
- [63] Chenglin Yang, Adam Kortylewski, Cihang Xie, Yinzhi Cao, and Alan Yuille. PatchAttack: A Black-box Texture-based Attack with Reinforcement Learning. In *European Conference on Computer Vision*, pages 681–698, 2020. 2, 3
- [64] Yichen Yang, Xiaosen Wang, and Kun He. Robust Textual Embedding against Word-level Adversarial Attacks. In *Proceedings of the Conference on Uncertainty in Artificial Intelligence*, page 2214–2224, 2022. 1
- [65] Zhen Yu, Xiaosen Wang, Wanxiang Che, and Kun He. TextHacker: Learning based Hybrid Local Search Algorithm for Text Hard-label Adversarial Attack. In *Proceedings of the Conference on Empirical Methods in Natural Language Processing (Findings)*, page 622–637, 2022. 1
- [66] Zhanyuan Zhang, Benson Yuan, Michael McCoyd, and David Wagner. Clipped bagnet: Defending against sticker attacks with clipped bag-of-features. In *2020 IEEE Security and Privacy Workshops (SPW)*, pages 55–61, 2020. 5
- [67] Alon Zolfi, Moshe Kravchik, Yuval Elovici, and Asaf Shabtai. The Translucent Patch: A Physical and Universal Attack on Object Detectors. In *Proceedings of the IEEE/CVF Conference on Computer Vision and Pattern Recognition*, pages 15232–15241, 2021. 2

6. Appendix

6.1. More Samples of Adversarial Patches

In this section, we provide more adversarial patches generated by GoogleAp, LaVAN, and VRAP in Fig. 9. As we can see, the adversarial patches generated by VRAP are much more realistic than GoogleAp and LaVAN and can act as real scrawls or logos, which validates our motivation.

6.2. More Samples of Physical Scrawls, Logos, and Adversarial Patches Crafted by VRAP

In this section, we provide more adversarial patches generated by VRAP that can be regarded as scrawls or logos in the real world. As shown in Fig 10, we craft the adversarial patches on ResNet-18 and place the adversarial patches in a natural position of victim images. In Fig. 10b, the original patch does not mislead ResNet-18. However, after adding natural adversarial patches in Fig 10c, ResNet-18 makes wrong decisions. The visually realistic adversarial patches validate that VRAP can be regarded as logos or scrawls in the real world and bring significant threats to deep models.

6.3. More Samples of Physical Adversarial Patches

In this section, we provide more adversarial patches employed in the real world. As shown in Fig 11, the adversarial patches generated by VRAP remains the visual reality of the original patches. Adversarial patches in Fig 11c successfully fool a ResNet-18 model, while the original patches in Fig 11b pose no impact on the ResNet-18 model. This validates that our proposed VRAP can be employed in the real world with high visual reality.

6.4. More Samples of Attention Heatmaps

In this section, we provide more heatmaps after adding original patches and adversarial patches. As shown in Fig 12, after adding adversarial patches, ResNet-18 is distracted by the adversarial patches, which is consistent with the results in Discussion.

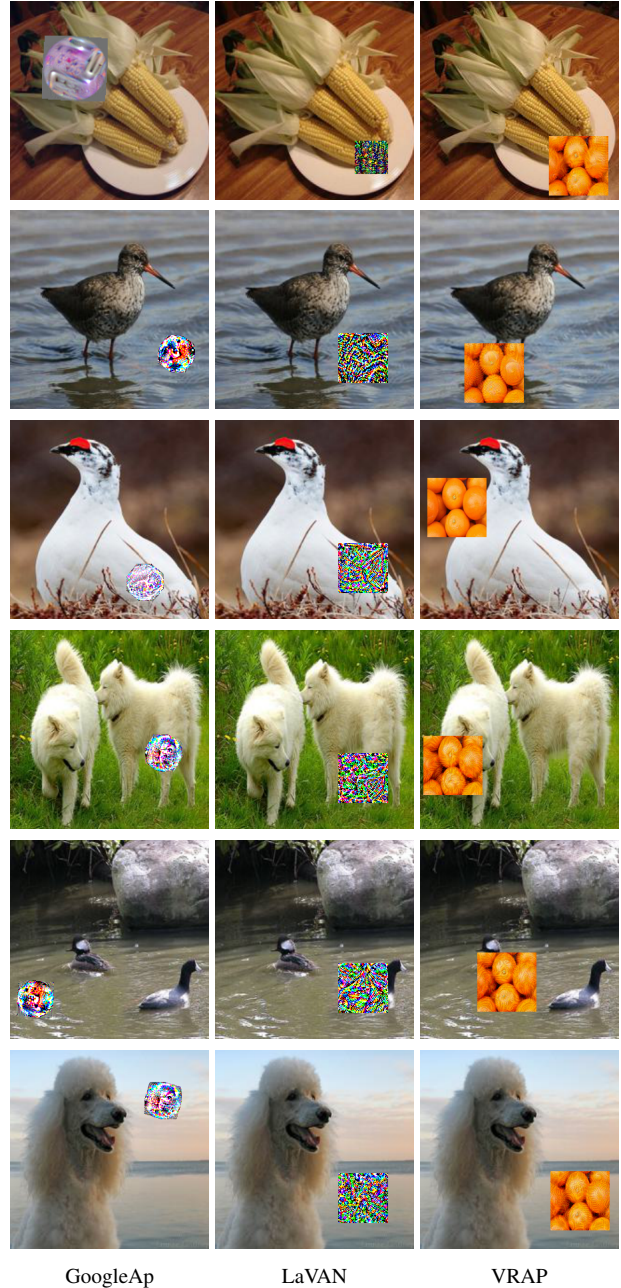


Figure 9. The adversarial patches w.r.t. the same input image generated by GoogleAp, LAVAN and our purposed VRAP, in which all the images are from ImageNet dataset.

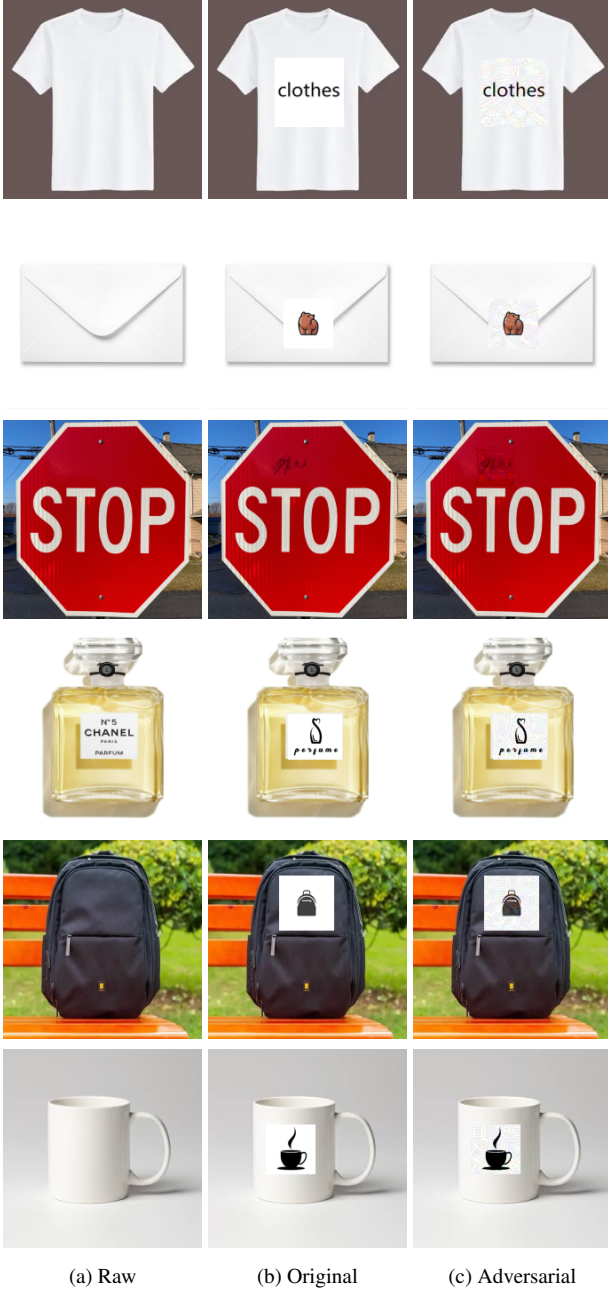


Figure 10. The raw images, images with original image patches and adversarial patches generated by VRAP on ResNet-18

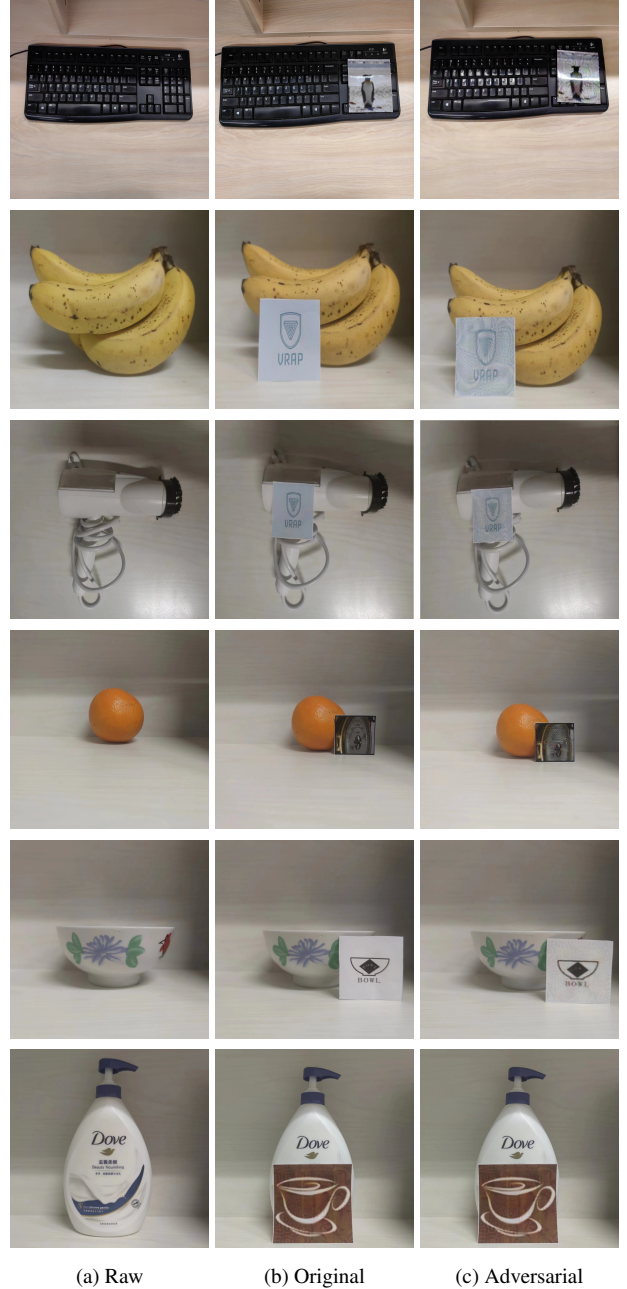


Figure 11. The raw images, images with original image patches, and adversarial patches in the physical world.

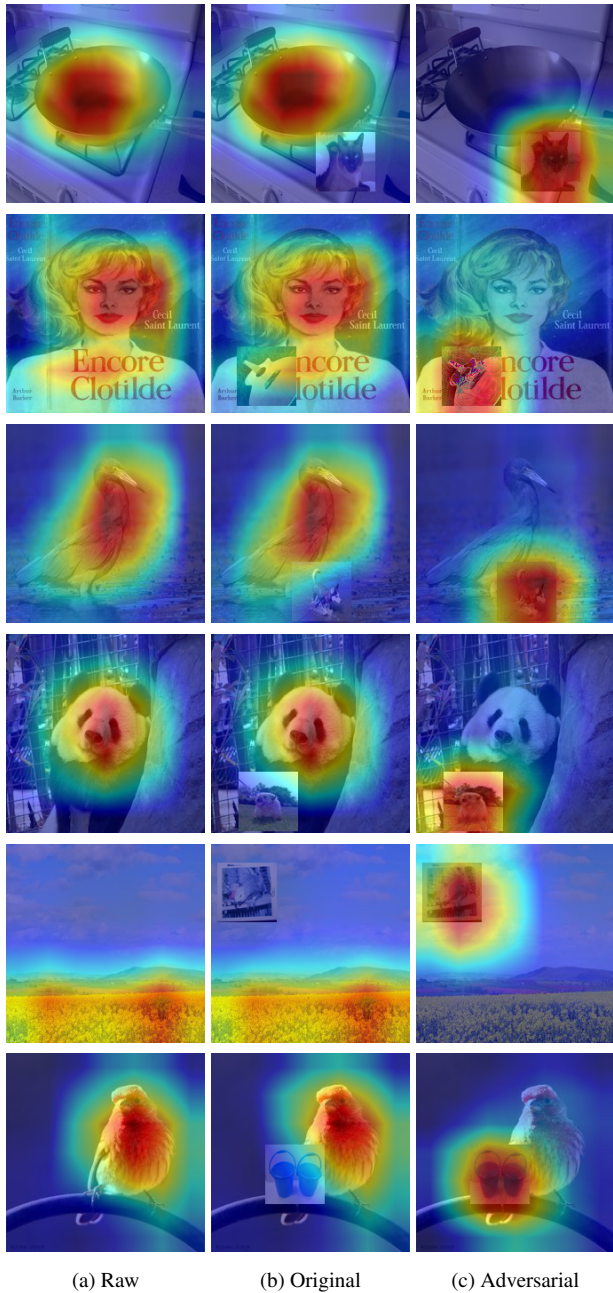


Figure 12. Attention heatmaps of raw image, the image with original patch and adversarial patches on ResNet-18.